AD-A119 818 SCIENCE APPLICATIONS INC ANNAPOLIS MD F/G 20/4
A NEW GENERALIZED CROSS-FLOW MOMENTUM INTEGRAL METHOD FOR THREE--ETC(U)
APR 82 C H VON KERCZEK N00014-81-C-0234
UNCLASSIFIED SAI-463-82-085-LJ NL

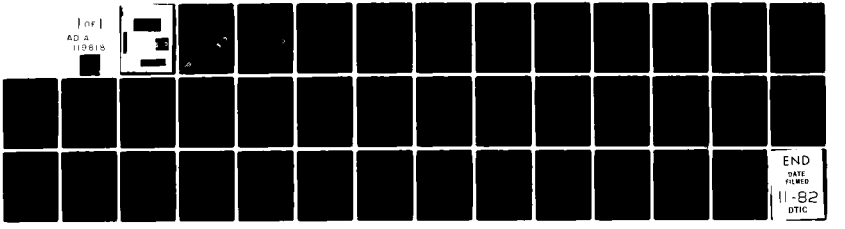

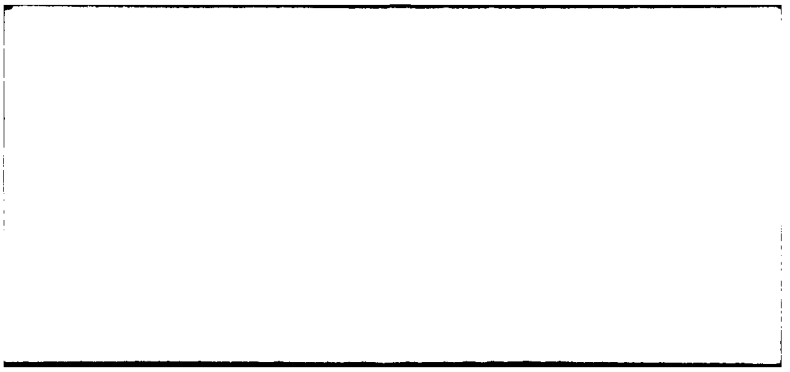

A NEW GENERALIZED CROSS-FLOW MOMENTUM INTEGRAL METHOD FOR THREE-DIMENSIONAL SHIP BOUNDARY LAYERS

DTIC
SELECTE
OCT 1 1982
D

DISTRIBUTION STATEMENT A
Approved for public release;
Distribution Unlimited

SAI
ATLANTA • ANN ARBOR • BOSTON • CHICAGO • CLEVELAND • DENVER • HUNTSVILLE • LA JOLLA
LITTLE ROCK • LOS ANGELES • SAN FRANCISCO • SANTA BARBARA • TUCSON • WASHINGTON

UNCLASSIFIED

SECURITY CLASSIFICATION OF THIS PAGE (When Data Entered)

REPORT DOCUMENTATION PAGE		READ INSTRUCTIONS BEFORE COMPLETING FORM
1. REPORT NUMBER SAI-463-82-085-LJ	2. GOVT ACCESSION NO. AD A119818	3. RECIPIENT'S CATALOG NUMBER
4. TITLE (and Subtitle) A NEW GENERALIZED CROSS-FLOW MOMENTUM INTEGRAL METHOD FOR THREE-DIMENSIONAL SHIP BOUNDARY LAYERS		5. TYPE OF REPORT & PERIOD COVERED Final - 3 Feb 1981 - 30 Jun 1982 6. PERFORMING ORG. REPORT NUMBER SAI-463-82-085-LJ
7. AUTHOR(s) C. H. von Kerczek		8. CONTRACT OR GRANT NUMBER(s) N00014-81-C-0234
9. PERFORMING ORGANIZATION NAME AND ADDRESS Science Applications, Inc. 134 Holiday Court, Suite 318 Annapolis, Maryland 21401		10. PROGRAM ELEMENT, PROJECT, TASK AREA & WORK UNIT NUMBERS
11. CONTROLLING OFFICE NAME AND ADDRESS David W. Taylor Naval Ship R&D Center Bethesda, Maryland 10084 (Code 1505)		12. REPORT DATE 2 April 1982 13. NUMBER OF PAGES ii + 30
14. MONITORING AGENCY NAME & ADDRESS(if different from Controlling Office) Office of Naval Research 800 N. Quincy Street Arlington, VA 22217		15. SECURITY CLASS. (of this report) UNCLASSIFIED 15a. DECLASSIFICATION/DOWNGRADING SCHEDULE

16. DISTRIBUTION STATEMENT (of this Report)

APPROVED FOR PUBLIC RELEASE; DISTRIBUTION UNLIMITED

DTIC ELECTE OCT 1 1982 S H

17. DISTRIBUTION STATEMENT (of the abstract entered in Block 20, if different from Report)

N/A

THIS RESEARCH WAS SPONSORED BY THE NAVAL SEA SYSTEMS COMMAND GENERAL HYDROMECHANICS RESEARCH PROGRAM ADMINISTERED BY THE DAVID W. TAYLOR NAVAL SHIP R&D CENTER, BETHESDA, MD 20084, (ATTN: CODE 1505)

19. KEY WORDS (Continue on reverse side if necessary and identify by block number)

GHR Program, Turbulence, Boundary Layers, Ships, Viscous Drag, 3-Dimensional

20. ABSTRACT (Continue on reverse side if necessary and identify by block number)

A new cross-flow model for a three-dimensional momentum integral turbulent boundary layer calculation method has been developed. This cross-flow model utilizes two parameters and is capable of representing the reversal (s-shaped) cross-flow profiles that do occur in ship boundary layers. The new method uses only an extra algebraic equation for determining the extra cross-flow parameter. The basic momentum integral equations used by the method are the streamwise and cross-flow momentum equations and the entrainment equation. The method has been programmed for calculating ship boundary layers.

DD FORM 1 JAN 73 1473 EDITION OF 1 NOV 65 IS OBSOLETE
S/N 0102-014-6601

UNCLASSIFIED

SECURITY CLASSIFICATION OF THIS PAGE (When Data Entered)

Certain higher order goemetric effects have been included. Test calculations for the experimental boundary layer data of the SSPA-Model 720 have been made The results are very promising. Good agreement with experimental data is obtained over that portion of the hull where viscous-inviscid interactions do not occur. Near the stern the predictions are qualitatively correct. The s-shaped, cross-flow profiles are predicted near the stern but they are somewhat inaccurate. The addition of viscous-inviscid interaction capabilities to the calculation should greatly improve the predictions of the boundary layer near the stern.

A NEW GENERALIZED CROSS-FLOW MOMENTUM INTEGRAL METHOD FOR THREE-DIMENSIONAL SHIP BOUNDARY LAYERS

SAI-463-82-085-LJ

Contract #N00014-81-C-0234

2 April 1982

Submitted to

David W. Taylor Naval Ship
Research & Development Center
Code 1505
Bethesda, MD

Submitted by

C. H. von Kerczek

SCIENCE APPLICATIONS, INC.

134 Holiday Court, Suite 318
Annapolis, Maryland 21401
(301) 266-0991; D.C. 261-8026

ABSTRACT

A new cross-flow model for a three-dimensional momentum integral turbulent boundary layer calculation method has been developed. This cross-flow model utilizes two parameters and is capable of representing the reversal (s-shaped) cross-flow profiles that do occur in ship boundary layers. The new method uses only an extra algebraic equation for determining the extra cross-flow parameter. The basic momentum integral equations used by the method are the streamwise and cross-flow momentum equations and the entrainment equation. The method has been programmed for calculating ship boundary layers. Certain higher order geometric effects have been included. Test calculations for the experimental boundary layer data of the SSPA-Model 720 have been made. The results are very promising. Good agreement with experimental data is obtained over that portion of the hull where viscous-inviscid interactions do not occur. Near the stern the predictions are qualitatively correct. The s-shaped cross-flow profiles are predicted near the stern but they are somewhat inaccurate. The addition of viscous-inviscid interaction capabilities to the calculation should greatly improve the predictions of the boundary layer near the stern.

Accession For	
NTIS GRA&I	☑
DTIC TAB	☐
Unannounced	☐
Justification	
By	
Distribution/	
Availability Codes	
Dist	Avail and/or Special
A	

DTIC COPY INSPECTED 3

TABLE OF CONTENTS

ABSTRACT	. . . . .	i
Section 1	INTRODUCTION	1-1
Section 2	CROSS-FLOW PROFILES	2-1
Section 3	A NEW CROSS-FLOW PROFILE	3-1
Section 4	THE BOUNDARY LAYER MOMENTUM INTEGRAL EQUATIONS	4-1
Section 5	NUMERICAL METHOD OF CALCULATION	5-1
Section 6	COMPUTATIONAL RESULTS	6-1
Section 7	CONCLUDING REMARKS	7-1
Section 8	REFERENCES	8-1

Section 1

INTRODUCTION

There have been several momentum integral methods formulated for calculating ship boundary layers (cf. ref. [1-6]). All these method have in common that the momentum integral equation along the potential flow streamlines, the entrainment equation and the momentum integral equation along the equipotential lines on the hull (the cross-flow equation) are solved numerically for the three main boundary layer parameters. These parameters are the streamline direction momentum thickness θ_{11}, the shape parameter H and the angle β between the surface shear stress vector and the potential flow streamlines. The minor differences (although they are important) between such momentum integral methods consist mainly of the empirical formulas that are used to relate the boundary layer parameters θ_{11}, H and β to the many other parameters that are required to describe completely the boundary layer. For example, the surface skin friction coefficient C_f is assumed to be related to the momentum thickness θ_{11} and shape factor H by an empirical formula. The skin friction formula used by various methods do not differ in a major way. There are also important differences among the methods in the way the equations are solved numerically. However, the differences in the numerical treatment are deemed to be technical and not fundamental ones.

The major fundamental difference among all the momentum integral ship boundary layer methods is in the way the cross-flow is handled. The standard way to deal with the cross-flow is to assume a cross-flow velocity profile shape in terms of certain directly relevant boundary layer parameters such as β. Then the main distinguishing feature of a method is the nature of the assumed cross-flow velocity profile.

This report describes the results of a research program that had several objectives. The first, most important objective was to develop a new cross-flow velocity profile that allowed the retention of the simplest form of

the momentum integral formulation (i.e., only three differential equations need be solved) but one that encompasses an adequate description of s-shaped profiles. Another objective was to develop a numerical method to solve the boundary layer equations which retained the basic streamline formulation but did not require a streamline-equipotential line grid system. Retaining the streamline formulation of the boundary layer equations is deemed important in cases when free surface effects must be taken into account. In such cases, the intersection of the free surface and the ship hull is a streamline which forms one boundary of the computational domain. However, it has been found [2] that the streamline-equipotential line grid is not a very good system for the numerical treatment of the boundary layer equations.

The third objective to include higher order geometric terms in the boundary layer equations is a required prelude to the development of a viscous-inviscid interaction method for more accurate calculation of the boundary layer close to the stern of a ship.

Section 2 of this report contains a brief review of various cross-flow velocity profiles that have been developed in the past. In Section 3 the new cross-flow profile developed in this research and its implementation is discussed. In Section 4 the boundary layer equations including the higher order geometric terms are given. Section 5 discusses the new numerical method for solving these equations. The results of the application of this method to the SSPA Model 720 [6,7] test case are described in Section 6.

Section 2

CROSS-FLOW PROFILES

The first moderately successful method for modeling the three-dimensional turbulent boundary layer was Mager's [8]. In this momentum integral method the cross-flow boundary layer velocity distribution v(z), where z is the coordinate normal to the boundary layer, was assumed to have the form

$$\frac{v}{U} = \frac{u}{U}\left(1 - \frac{z}{\delta}\right)^2 \tan\beta \qquad (1)$$

where U is the potential flow velocity at the edge of the boundary layer (hereafter called the slip velocity), u(z) is the boundary layer velocity distribution in the inviscid streamline direction and δ is an overall boundary layer thickness. The velocity profile (1) has become known as the Mager profile and it is still the basis of most of the simpler three-dimensional turbulent boundary layer calculation methods. The basis of this profile is only three boundary conditions. Profile (1) satisfies the condition that the cross-flow velocity is zero at the wall and the edge $z = \delta$ and that the limting streamline makes the angle β with respect to the inviscid streamline, i.e.,

$$\lim_{z \to 0} \frac{v}{u} = \tan\beta \ . \qquad (2)$$

The only unknown parameter of the Mager profile (1) is the angle β. Hence, the single cross-flow momentum equation is sufficient to determine β.

It has been recognized by most researchers of three-dimensional boundary layers that the profile (1) is unsuitable for describing cross-flow velocity distributions that often occur in regions just downstream of streamline inflection points. For example, it has been found often [4,7] that the cross-flow profile is s-shaped in certain regions on ship hulls. The profile (1) is of one sign across the boundary layer from $z = 0$ to $z = \delta$. Hence, it cannot describe s-shaped profiles. In order to encompass the variety of

profile shapes that do occur, it seems evident that the cross-flow profile requires for description more parameters than just β. With the addition of each extra parameter to the cross-flow profile an extra equation is required to determine this parameter. The addition of such equations often complicates the momentum integral method to the point where the differential boundary layer equations are as easily solved. Furthermore, each additional equation requires additional experimental data for closure.

There have been many multiparameter cross-flow profiles developed. The most extensive set of these profiles was developed by Eichelbrenner [9]. A similar set was developed by Shanebrook and Hatch [10]. The three-dimensional boundary layer methods based on these profiles have not proved to be any more accurate than the simple Mager method [11]. The reason for this may be that these profile families rely on parameters which are related to the slope of the velocity profile at the outer edge of the boundary layer. It is difficult to obtain reliable test data on which to base a differential equation that governs the behavior of such parameters.

Okuno [5] developed a cross-flow profile that simply multiplies the Mager profile (1) by a linear function of z/δ. This linear function has one free parameter which is determined by the cross-flow moment of momentum integral equation. New unknown boundary layer quantities, such as the moment of the shear stress, are introduced by this equation. Empirical data is lacking for such terms. Hence, the range of usefulness of such an equation is limited. Okuno does show that his method gives better predictions than Mager's profile of the cross-flow near the stern of a ship model. Although this method is an improvement over Mager's method, the gain seems slight in comparison to the increase in complexity introduced by the cross-flow moment of momentum integral equation.

It seems that the construction of two parameter cross-flow profiles such as Eichelbrenner [9] and Okuno's [5] do not capture the essential physical mechanism that governs the cross-flow in the boundary layer. In the next section of this report the proper physical model of the cross-flow is described.

A two parameter cross-flow profile and a simple algebraic governing equation for the extra parameter is then synthesized based on this model.

Section 3

A NEW CROSS-FLOW PROFILE

The driving force of the boundary layer cross-flow is the geodesic curvature of the inviscid streamline on the surface of the hull. This dimensionless curvature term, denoted here by K_2, acts as a negative pressure gradient in a direction to the concave side of the streamline. Since the velocity in the boundary layer is diminished from the free stream velocity, the fluid particles there have insufficient momentum to withstand this pressure gradient. Thus, they tend to flow down the pressure gradient, that is towards the concave side of the streamline. The fluid particles nearest the ship surface have the least momentum. Hence, a change in sign of K_2 causes these particles to reverse rapidly their direction of motion. The fluid particles away from the immediate vicinity of the ship surface are less constrained. The prolonged application of a pressure gradient K_2 to these particles endows them with sufficient momentum that a reversal of the sign of K_2 will result in a belated reversal of the direction of motion of these particles. The disparity in the response to changes of the sign of the cross-flow pressure gradient K_2 causes the development of s-shaped velocity profiles downstream of streamline inflection points ($K_2 = 0$). It is important to note that the inner part of the boundary layer velocity responds quickly to the changes in sign of the pressure gradient K_2. In fact, a careful observation of the values of β measured in the experiments of Reference 7 and the calculated values of K_2 shows them to be fairly closely correlated. The angle β is a direct measure of the direction of the velocity of the inner boundary layer particles.

The cross-flow momentum equation governs the momentum flux defect $U^2\theta_{21}$ of the cross-flow. The major contribution to this momentum flux comes from the outer part of the boundary layer. This suggests that the cross-flow velocity profile consists of an extensive outer region which is characterized by the parameter θ_{21}. In addition to this outer region of the cross-flow there is a small inner region which is characterized by the parameter β.

Furthermore, the cross-flow velocity profile must satisfy the same boundary conditions that were satisfied by Mager's profile (1). The following profile is suggested:

$$\frac{v}{U} = \frac{u}{U}\left(1-\frac{z}{\delta}\right)^2\left[\left(1-\frac{I_1}{I_2}\frac{z}{\delta}\right)\tan\beta - \frac{\theta_{21}}{I_2\delta}\frac{z}{\delta}\right] \tag{3}$$

where

$$I_1 = \int_0^1 \frac{u}{U}\left(1-\frac{z}{\delta}\right)^2 d\left(\frac{z}{\delta}\right)$$

and

$$I_2 = \int_0^1 \frac{u}{U}\left(1-\frac{z}{\delta}\right)^2\left(\frac{z}{\delta}\right) d\left(\frac{z}{\delta}\right).$$

The cross-flow velocity profile (3) satisfies identically the definition of the cross-flow momentum thickness

$$\theta_{21} = -\int_0^\delta \frac{uv}{U^2}\, dz. \tag{4}$$

The term proportional to θ_{21} in equation (3) gives the main part of the cross-flow profile. The term proportional to $\tan\beta$ in equation (3) corrects the inner part of the profile to acquire the correct direction there ($\tan\beta$). Equation (3) encompasses certain s shapes under the condition that $\tan\beta$ and θ_{21} have the same sign.

The cross-flow momentum integral equation governs the distribution of the quantity θ_{21} along the streamlines on the hull. It has already been explained that the velocity of the fluid particles in the wall region of the boundary layer responds directly to the local value of the cross-flow pressure gradient K_2. Thus, it is postulated that $\tan\beta$ satisfies the simple equation

$$\tan\beta = cK_2 - (1-c)\frac{\theta_{21}}{\delta I_1} \tag{5}$$

where c is a coefficient to be determined by comparision of the results using this equation with experimental results. The value of $c = 0$ reduces the profile (3) to Mager's profile (1) and reduces the equation (5) to the same relationship between $\tan\beta$ and θ_{21} that is obtained using Mager's profile.

Equation (5) properly accords with the various ways in which the cross-flow may occur. For example, a two-dimensional boundary layer may be suddenly perturbed by a lateral motion of the boundary. Then θ_{21} is initially zero and the lateral velocity of the boundary can be related to an effective value of K_2. In the initial instance of such a perturbation the value of $\tan\beta$ is, in fact, directly proportional to K_2. On the other hand, the boundary layer may develop first along curved stramlines and then flow onto straight streamlines for which $K_2 = 0$. The boundary layer cross-flow will then be proportional to θ_{21} alone as modeled by equation (5). In fact, if the streamwise pressure gradient is adverse along straight streamlines then the cross-flow thickness θ_{21} will grow in magnitude even with $K_2 = 0$. This condition is encompassed by equation (5). Note that the opposite signs of θ_{21} and $\tan\beta$ are a consequence of the definition (4). An interesting phenomenon is that the cross-flow thickness can grow even after K_2 changes sign and the inner part of the cross-flow is driven in the opposite direction to the outer part. This may happen in an adverse streamwise pressure gradient. In fact this occurs at the stern of ships and is the main cause of the strongly s-shaped cross-flow velocity profiles there.

Section 4

THE BOUNDARY LAYER MOMENTUM INTEGRAL EQUATIONS

It is not necessary to give the detailed derivation of the boundary layer equations because this derivation is tedious though elementary. Instead, only the final equations are given and all the terms are explained in detail. The classical three-dimensional momentum integral equations which do not contain the higher order geometric terms can be found in many sources (for example, references [1-5]). The modified momentum integral equations that include geometric correction factors will be given in terms of the thin boundary layer thicknesses (such as momentum thickness and displacement thickness) instead of the thick boundary layer parameters such as momentum area, displacement area, etc. The reason for this is most of the auxiliary experimental data that is needed to close the system of equations is given in terms of the classical thicknesses. The conversion between the thicknesses and areas is entirely trivial as long as the surface curvature is not zero. However, when the curvature is zero, the momentum area, etc., are undefined (when these are originally defined in terms of the local radius of curvature, as for a body of revolution). Regions on the surface for which the total curvature is zero are extensive on most ships; namely flat sides and bottoms. Thus, it is convenient for ship applications to deal directly with thicknesses.

Let s be the arc-length coordinate along an inviscid surface streamline. Let p be the arc-length along a surface equipotential line. The momentum integral equation along the streamlines is

$$\frac{\partial \theta_{11}}{\partial s} = \tfrac{1}{2}\alpha C_{f1} - \theta_{11}\left(\frac{2 + \rho H}{U}\frac{\partial U}{\partial s} - \alpha K_1\right) - \alpha \frac{\partial \theta_{12}}{\partial p} \quad . \tag{6}$$

The boundary layer entrainment equation is

$$\frac{\partial q}{\partial s} = (\gamma + \varepsilon)\, F(G) - q\left(\frac{1}{U}\frac{\partial U}{\partial s} - \gamma K_1\right) + \gamma \frac{\partial \delta_2}{\partial p} \, . \tag{7}$$

The cross-flow momentum integral equation is

$$\frac{\partial \theta_{21}}{\partial s} = \tfrac{1}{2}\omega C_{f2} - 2\theta_{21}\left(\frac{1}{U}\frac{\partial U}{\partial s} - \omega K_1\right) - \theta_{11}(1 + H)\omega K_2 \ . \tag{8}$$

The factors K_1 and K_2 are the geodesic curvatures of the equipotential lines and streamlines respectively. The entrainment parameter q is defined by

$$q = G\theta_{11} \tag{9}$$

where G is Head's shape factor. Head's shape factor G is related to H empirically. The empirical data will be given later. The boundary layer thicknesses are defined as follows:

$$\theta_{11} = \int_0^\delta \left(1 - \frac{u}{U}\right)\frac{u}{U}\,dz \tag{10a}$$

$$\delta_1 = \int_0^\delta \left(1 - \frac{u}{U}\right)\,dz \tag{10b}$$

$$\theta_{12} = \int_0^\delta \left(1 - \frac{u}{U}\right)\frac{v}{U}\,dz \tag{10c}$$

$$\delta_2 = -\int_0^\delta \frac{v}{U}\,dz \ . \tag{10d}$$

The shape factor H is defined by the equation

$$H = \delta_1/\theta_{11} \ . \tag{11}$$

The terms C_{f1} and C_{f2} are the surface skin friction coefficients in the streamline and equipotential line directions respectively. Equation (2), which defines tanβ, implies that

$$C_{f2} = C_{f1}\tan\beta \ . \tag{12}$$

The function F(G) is the entrainment rate. It is given empirically. The terms α, ρ, γ, ε and ω are the higher order geometric correction factors.

Let $\vec{i}$ be the unit vector in the direction opposite to the ship velocity. Let $\vec{e}_s$ be the unit vector tangent to a surface streamline and let $\vec{e}_p$ be the unit vector tangent to a surface equipotential line. Then by definition

$$K_1 = \vec{e}_s \cdot \frac{d\vec{e}_p}{dp} \tag{12a}$$

$$K_2 = \vec{e}_p \cdot \frac{d\vec{e}_s}{ds} . \tag{12b}$$

The geometric parameters α, ρ, γ, ε and ω are defined by

$$\alpha = \frac{h}{h + \tau\delta} \tag{13a}$$

$$\gamma = \frac{h}{h + \mu\delta} \tag{13b}$$

$$\omega = \frac{h}{h + \sigma\delta} \tag{13c}$$

$$\rho = \frac{h + \delta/(n+1)}{h + \delta\tau} \tag{13d}$$

$$\varepsilon = \frac{\delta}{h + \mu\delta} \tag{13e}$$

and the factor h is the normal radius of curvature of a surface equipotential line. This normal radius of curvature is defined by

$$h^{-1} = (\vec{e}_s \times \vec{e}_p) \cdot \frac{d\vec{e}_p}{dp} . \tag{14}$$

The terms τ, μ and σ in equations (13a-e) are defined by

$$\delta\theta_{11}\tau = \int_0^\delta \left(1 - \frac{u}{U}\right) \frac{u}{U} \, z\,dz \tag{15a}$$

$$\delta q\mu = \int_0^\delta \frac{u}{U} \, z\,dz \tag{15b}$$

$$\delta\theta_{21}\sigma = -\int_0^\delta \frac{uv}{U}\, z\,dz \ . \qquad (15c)$$

The geometric terms α, ρ, γ, ε and ω that are included in equations (6)-(8) are approximations of the most important terms that occur in the integrals of the boundary layer when the variations of the coordinates in the direction normal to the surface are accounted for.

The following empirical data is used to close the system of equations (6)-(8). This data is based on Head's [12] entrainment method for turbulent boundary layers. The streamwise skin friction coefficient C_{f1} is given by the formula

$$C_{f1} = \exp(CH + B) \qquad (16a)$$

$$C = 0.019521 + D(-0.386768 + D(0.028345 - 0.000701D)) \qquad (16b)$$

$$B = 0.191511 - D(0.83489 + D(-0.062588 + 0.001953D)) \qquad (16c)$$

$$D = \ln(R_L U \theta_{11}) \qquad (16d)$$

The rate of entraimnent function F(G) is given by the formula

$$F(G) = 0.0306(G - 3.0)^{-0.653} \qquad (17)$$

where

$$G = 1.535(H - 0.7)^{-2.715} + 3.3 \ . \qquad (18)$$

The cross-flow velocity profile has been given by equation (3). The coefficient c in equation (5) is given tentatively the value

$$c = 0.125 \qquad (19)$$

This value for c seems to give promising results in the test calculation for the SSPA-Model 720. However, an extensive program of calculation and comparison

with the many sets of ship model boundary layer measurements that are available should be undertaken before a definitive value of this coefficient is established.

The cross-flow boundary layer thickness δ_2 and θ_{12} can be obtained in terms of parameters θ_{11}, H, β and θ_{21} by making use of the cross-flow velocity profile (3), the definitions (10c, d) and the following streamwise velocity profile u/U (see Kool [13]):

$$\frac{u}{U} = [1 - E(1 - \frac{z}{\delta})^n](1 - e^{-Qz^+}) \tag{20a}$$

where

$$E = 1 - 22e^{-H/2}\sqrt{C_{f1}} \tag{20b}$$

$$Q = \tfrac{1}{2}C_{f1}/(1 - E) \tag{20c}$$

$$z^+ = \frac{zR_\delta}{\delta} \tag{20d}$$

$$R_\delta = R_L \frac{\delta}{L} \tag{20e}$$

$$n = \frac{1}{H - 1} \tag{20f}$$

where L is the scale length of the ship, $R_L = (U_\infty L)/\nu$ is the Reynolds number, U_∞ is the forward speed of the ship and ν is the kinematic viscosity of the water.

Equations (3)-(20) establish a sufficient amount of information to calculate the underwater boundary layer on a ship hull if the ship hull geometry and the inviscid flow around the hull are specified. These items are discussed in the next section on the numerical method used to solve the boundary layer equations (6)-(8). Certain terms involving the square of the cross-flow velocity have been dropped from these equations because they are negligibly small. See references [1-6] for the complete boundary layer momentum integral equations.

Section 5

NUMERICAL METHOD OF CALCULATION

The numerical problem of calculating the boundary layer consists of computing the inviscid flow field about the ship hull and then numerically integrating the three first-order partial differential equations (6)-(8) along the streamlines. This report is concerned only with the boundary layer problem so it is assumed that the inviscid flow field for zero Froude number flow (the flow about the double model) is known. It is desirable to have a versatile method for calculating the boundary layer that keeps the calculation of the inviscid and viscous flow fields as independent as possible. Hence it is assumed that the values of the inviscid velocity are given at a set of NP points on each of M cross-sections of the hull. The number NP may vary from one cross-section to another. The hull surface is described by a modified form of the mapping method of von Kerczek and Tuck [14]. Let x, y, z be the coordinates in the longitudinal, lateral and vertical directions with respect to the centroid of the ship's design load waterplane. The positive x axis is in the direction of the stern of the ship. The part of the ship hull below the water is described by the following surface equation:

$$\vec{R}(x,\theta) = x\vec{i} + y(x,\theta)\vec{j} + z(x,\theta)\vec{k} \tag{21}$$

where $(\vec{i},\vec{j},\vec{k})$ is the set of unit vectors in the x, y, z directions respectively. The functions $y(x,\theta)$ and $z(x,\theta)$ are derived from the following mappings of a cross-section of the hull onto the lower half of the unit circle in the θ-plane. The first mapping is the bilinear fraction power map

$$\frac{w - b}{w + b} = \left(\frac{\zeta - b}{\zeta + b}\right)^{1/\alpha} \tag{22}$$

where $b = b(x)$ is the starboard load waterline profile, $\alpha = 2(1 - \pi/\Gamma)$, Γ is the angle the load waterline tangent of the cross-section makes with respect to the horizontal y-axis, $\zeta = y + iz$, $i = \sqrt{-1}$ and w is an auxiliary complex plane. The

purpose of this mapping is to straighten the angle Γ to be 90^0 in the w-plane. Then the mapped cross-section in the w-plane is mapped onto the unit circle in the f-plane by the method of von Kerczek and Tuck [14] as follows:

$$w = \sum_{n=1}^{N} a_n f^{3-2n} \tag{23}$$

where Re f = 0 and Im f = θ. The coefficients a_n, n=1, ..., N, the half-beam b and the exponent α are all computed for a number, say K, of stations along the hull. These values are then interpolated along the hull using cubic Hermite polynomial splines in which the first derivative with respect to x is continuous. This description of the hull surface alleviates the two main inaccuracies associated with the method of von Kerczek and Tuck [14]. The fractional mapping (22) allows any waterline slope instead of only the vertical slope allowed by the method of von Kerczek and Tuck [14]. The cubic Hermite spline lengthwise interpolation of a_n's, α and b considerably reduces the hull waviness that results from the high degree of polynimial interpolation of the von Kerczek and Tuck [14] method.

The availability of the surface equation representation (21) of the hull provides a natural intrinsic surface coordinate system. This system is made up of longitudinal lines of constant θ and the cross-sections x = constant. This surface coordinate system is very nearly orthogonal (see reference 2). It is visibly non-orthogonal only very close to the bow and stern of ordinary ships such as the SSPA model 720. On a parallel middle body this surface coordinate system is orthogonal.

The boundary layer equations (6)-(8) are solved on a rectangular grid in the x-θ plane that covers the underwater portion of the hull surface. However, these equations are integrated locally along the streamlines. The method of this calculation can be illustrated by reference to Figure 1 which shows the rectangular grid in the x-$^{\circ}$ plane

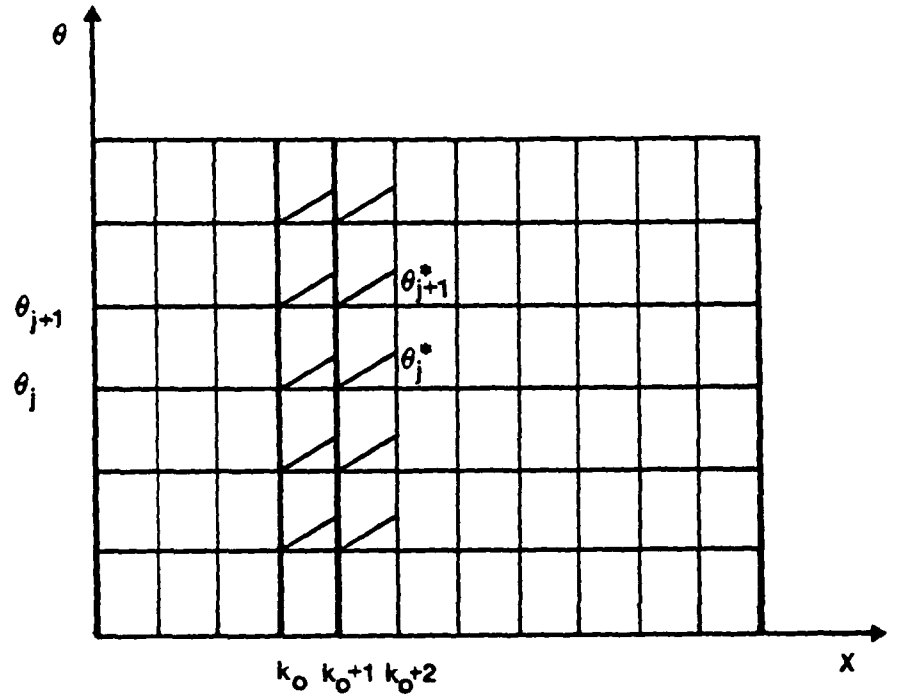

Figure 1. Schematic of grid in the x-θ plane showing streamline segments along which boundary layer equations are integrated.

The boundary layer calculation procedure begins at a station x_0, designated as $k = k_0$. There the primary boundary layer parameters θ_{11}, q and θ_{21} are given (say by experiments) on a set of points θ_j. The given values of θ_{11}, q and θ_{21} are sufficient to calculate the values of all the other required boundary layer parameters using the various formulas of Section 4.

The inviscid flow velocity is known at the cross-section k_0 on some other set of points. These values of the inviscid velocity are first interpolated with respect to the coordinate θ, using cubic Hermite splines, onto the points θ_j. These values of the inviscid velocity are then used to calculate the segments of the streamlines that pass through the points θ_j at station k_0 and intersect the cross-section at $k_0 + 1$ at the points designated by the θ_j^* as shown in Figure 1. The inviscid velocity at station $k_0 + 1$ is then interpolated to the streamline intersections. Equations (6)-(8) can now be integrated along the streamline segments from the points θ_j at station k_0 to the respective streamline intersections at the station $k_0 + 1$. The integration

method that has been used for this purpose is one that evaluates the cross-derivatives $\partial\delta_2/\partial p$ and $\partial\theta_{12}/\partial p$ at station k_o. Then equations (6)-(8) are integrated forward one step as ordinary differential equations, with respect to s, using a perdictor corrector method based on the Euler and Trapezoidal integragion rules (see, for example, reference 15). After the values of θ_{11}, q and θ_{21} have been calculated at the streamline intersection points at station $k_o + 1$, these values are interpolated, again using cubic Hermite splines, onto the points θ_j. The procedure can then be carried out exactly in the same way to integrate the equations (6)-(8) from station $k_o + 1$ to $k_o + 2$, and so on to the end of the ship.

This method has proved to be very easy to implement and has the following convenient features. The number and distribution of integration points θ_j at each station can be changed easily at every step. This can accommodate regions of rapid changes of the boundary layer parameters and allows marching around local regions of separation. Either or both of the side boundaries (in the example shown in Figure 1, the keel and load waterline) can be boundary streamlines and need not follow a line of constant θ. For example, if the complete ship problem is treated in which the free surface is not assumed to be flat, then the load waterline streamline is replaced by the free surface streamline. The boundary layer calculation method does not have to be carried out on the same set of points as the ones at which the inviscid velocity is specified. The only requirement is that the inviscid velocity is specified at some set of points on each cross-section k. This can be accomplished easily by a suitable interpolation preprocessing of whatever inviscid velocity data is provided (for example, by a Hess-Smith type of calculation).

The above description of the calculation procedure focused directly on the main elements of the numerical method for integrating the equations (6)-(8) along the surface of the hull. No mention was made of the calculation of all the geometric data such as K_1, K_2, h, dp, ds, directional unit vectors and inviscid velocity gradients in order to keep the discussion as simple as possible. The required geometric and pressure gradient data is fairly easy to calculate using the surface equation (21). For example, the unit vector $\vec{e}_n$ normal

to the surface is calculated directly by analytically differentiating the surface equation (21). The unit vector $\vec{e}_s$ tangent to a streamline is easily calculated using the inviscid velocity. Then the unit vector $\vec{e}_p$ along the surface equipotential lines is calculated by

$$\vec{e}_p = \vec{e}_n \times \vec{e}_s \quad . \tag{24}$$

The arclength increments ds and dp are easily determined using the surface equation (21) and the vectors $\vec{e}_s$ and $\vec{e}_p$. The the derivatives $\partial U/\partial s$, $d\vec{e}_s/ds$ and $d\vec{e}_p/dp$ are calculated by difference approximations. These calculations are very similar to the ones described in reference 2. The reader is referred to this reference for the details.

The important aspect of this boundary layer calculation method that makes possible a fairly easy way of calculating all the required surface geometry is the representation of the ship hull surface by the conformal mapping functions. This method of representing the hull surface has been discussed in detail in reference 14. However, the modification using the fraction power mapping (22) is new so that it is worthwhile to discuss briefly why this mapping is used and the improvements that are gained in the surface representation. This can be illustrated best by referring to Figure 2. This figure shows the given input offsets for station x = +0.9L, where L is the half-length between perpendiculars, of the SSPA-Model 720 and the representation of this station by the conformal mapping method with and without the preliminary mapping (22). The mapping (23) used N = 7 coefficients in both cases. The vertical slope at the load waterline (z = 0) of the section representation without the mapping (22) cannot be eliminated by choosing larger values of N. It is easy to see that by using the preliminary mapping (22) the representation of the section is dramatically improved.

This numerical method has been implemented in the computer program. The detailed description of this implementation is left for an appropriate Program Manual. The next section describes the results of a test calculation for the SSPA-Model 720.

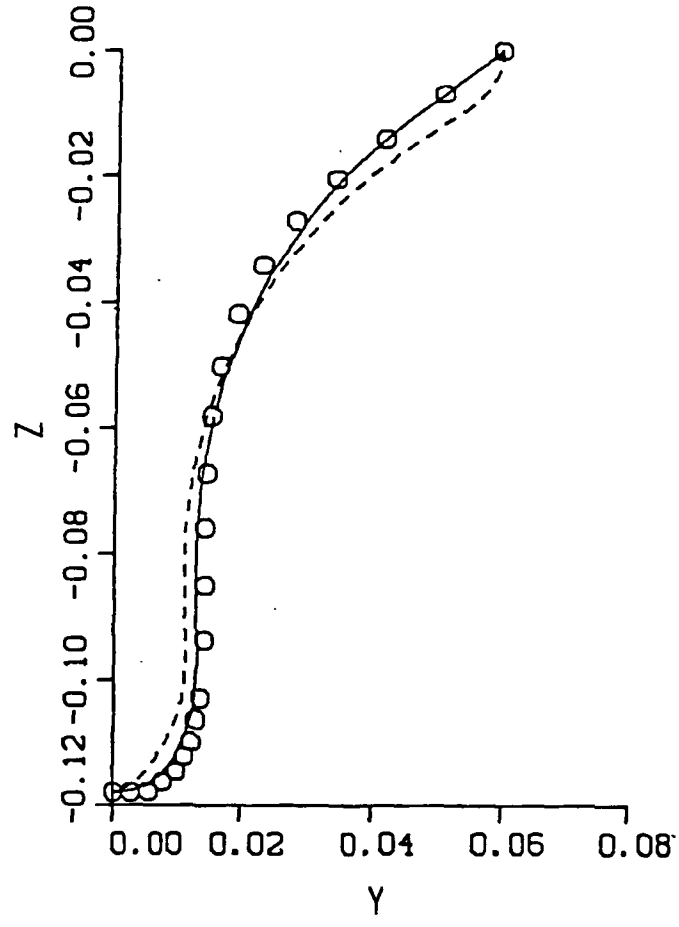

Figure 2. Comparison of the mapping representation of section x = 0.9L of the SSPA-Model 720 with input offsets. The input offsets are the circles. The dashed curve (-----) is the representation by the mapping formula (23) alone. The solid curve (———) is the representation by the combined mapping formulas (22) and (23).

Section 6

COMPUTATIONAL RESULTS

The boundary layer calculation method described in Section 3 through 5 was programmed and tested on the SSPA-Model 720. This is a double model of a moderate block coefficient (C_B = 0.675) cargo hull. Extensive boundary layer measurements were made on this model by Larsson[6]. This model was used as one of the test cases to which many different boundary layer calculation methods have been applied in the SSPA-ITTC Workshop on Ship Boundary Layers[7]. Reference to the Workshop report[7] can be made for all the details of the model and the experimental data, as well as the comparison of the performance of various boundary layer calculation methods.

The computed boundary layer by the present method will be compared with the experimental data for the SSPA-Model 720. No direct comparisons of the present method with any of the other methods presented at the Workshop will be made because this would require too much replotting of the published data. Reference to the report[7] can be made to compare the present method with the others of the Workshop.

The present boundary layer calculation method requires, like all other methods, the specification of certain boundary layer parameters along an initial cross-section of the hull. The boundary layer can then be computed for stations downstream of the starting cross-section. The present calculation method requires the specification of four boundary layer parameters at the starting station. The most convenient parameters to be specified are the streamwise momentum thickness θ_{11}, the shape factor H, the cross-flow angle β and the cross-flow momentum thickness θ_{21}. However, starting data at station x = -0.5L, where L is the half-length between perpendiculars and the origin of x is at midship, given in reference 7 is the distribution of θ_{11}, H and β only. Hence the starting distribution of the values of θ_{21} were estimated on the basis of the relationship

$$\theta_{21} = -\delta I_1 \tan\beta \qquad (24)$$

(see equation 5). Equation (24) is the result of assuming that the Mager cross-flow velocity profile (1) is valid. This approximation for the initial distribution of θ_{21} may be responsible for part of the discrepancy between the computed and the measured boundary layer characteristics discussed below.

The boundary layer downstream of station x = -0.5L was computed for a dense set of points on the hull surface (see Figure 1). It is simplest to discuss the results by comparing them with measured data along certain curves on the surface of the hull. The first set of comparisons between computed and experimental results is the distrubition of values of θ_{11} and β along two streamlines, designated streamlines B and C (see reference 7). Streamline B runs down the hull close to the keel except near the stern where it turns upward across the bilge towards the location where the propeller shaft would emerge from the hull. Streamline C runs down the hull on the center of the bilge and emerges at the stern from the hollow beneath the stern section flare. Figure 3 gives a comparison between the distribution of computed and experimental values of the streamwise momentum thickness θ_{11} along streamlines B and C. This figure also shows the experimental values of θ_{11} along the keel, designated as streamline A, for comparison with the values of θ_{11} along streamline B. Direct calculation of the boundary layer along the keel was not made. It can be seen in Figure 3 that the values of θ_{11} are well predicted by the present method on streamline C, but on streamline B the values of θ_{11} are considerably overpredicted. Calculations of the boundary layer were also made using a small cross-flow approximation to equations (6)-(8). In this approximation the terms involving θ_{12} and δ_2^* in equations (6) and (7), respectively, are dropped. The cross-flow has no effect on the streamwise flow in this approximation. The resulting distribution of values of θ_{11} along streamline B is not substantially different from the values shown in Figure 3. Hence the overprediction of the values of θ_{11} on streamline B cannot be attributed to cross-flow effects. It seems likely that the values of the pressure gradients along streamline B calculated by the present method may be larger than

the actual values in the experiment. The results shown in Figure 3 are very encouraging though.

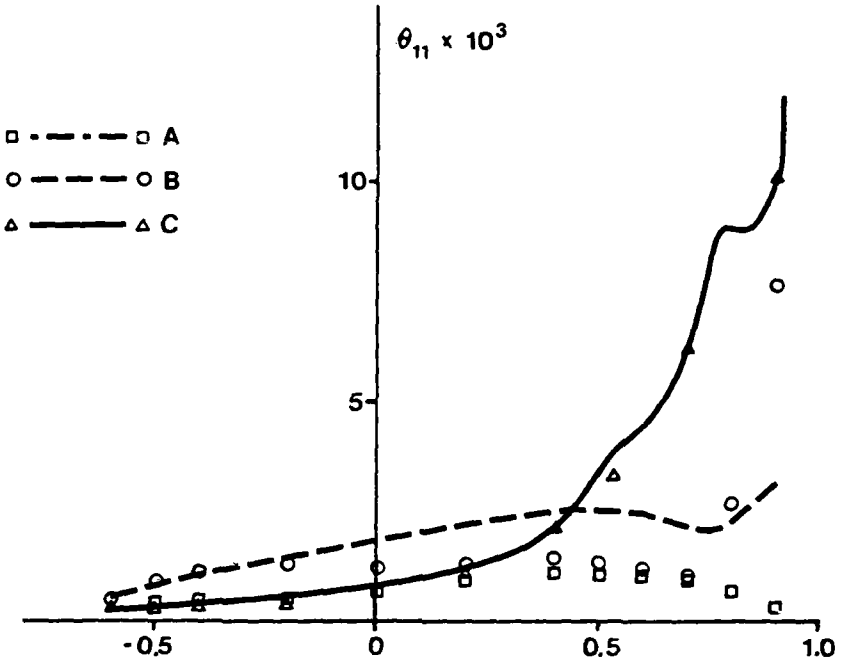

Figure 3. Comparison of the experimental and computed values of the streamwise momentum thickness θ_{11} along streamlines B and C on the SSPA-Model 720. The curves are the computed values and the points are the experimental values of θ_{11}.

Figure 4 gives a comparison of the distribution of computed and experimental values of the cross-flow angle β along streamlines B and C. Here the similarity between the computed and experimental results is heartening. The discrepancy between the computed and measured values of β near the starting station $x = -0.5L$ on streamline B may be due to the possibly inaccurate initial values of θ_{21} estimated by using formula (24). It should be noted that most of the values of β are fairly small. The measured values of β were obtained by measuring the inner part of the boundary layer velocity profiles using a Preston tube[6]. The calibration and even the applicability of this

technique for measuring the flow direction close to the wall is uncertain. Hence, a precise similitude between the computed and measured values of should not be expected.

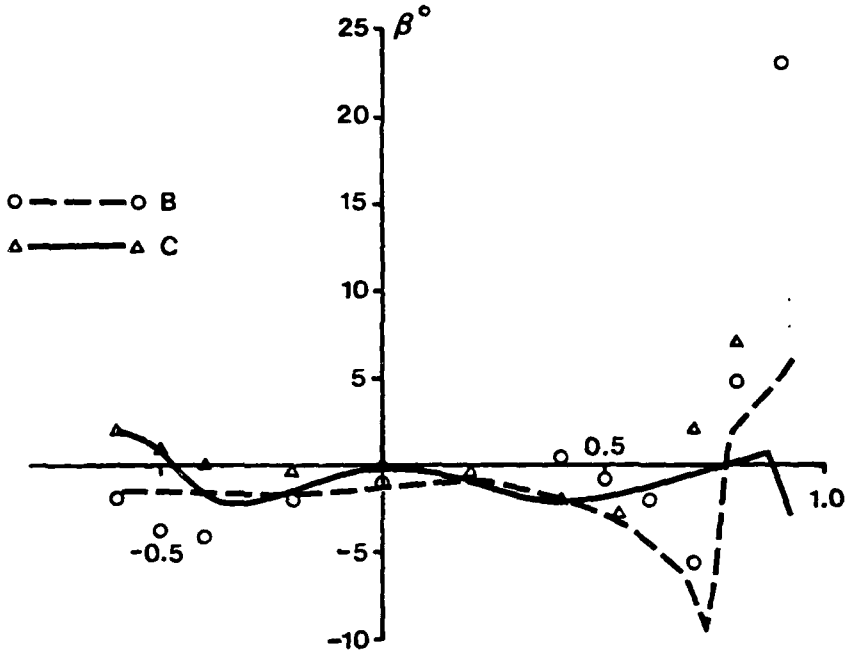

Figure 4. Comparison of the experimental and computed values of the cross-flow angle β along the streamlines B and C on the SSPA-Model 720. The curves are the computed values and the points are the experimental values.

Figures 5, 6 and 7 show the distribution of values of θ_{11} and β on the cross-sections at x = 0.5L, 0.7L and 0.9L, respectively. The computed and measured values of θ_{11} and β are in satisfactory agreement at station x = 0.5L. At station x = 0.7L the comparison between the computed and measured values is less satisfactory but not too bad. At station x = 0.9L the computed values of θ_{11} and β are only qualitatively similar to the respective measured values. The main part of the discrepancies between computed and measured values of θ_{11} and β shown in Figures 6 and 7 is most likely due to the occurrence of viscous-inviscid interactions that have not been accounted

for in the present computational method. A second factor causing this discrepancy may be the very poor resolution of the given pressure distribution near the keel at station x = 0.9L. The interpolation near the keel of the potential flow data given by the Workshop is very erratic. This causes the values of β to be negative and very large in magnitude near the keel at station x = 0.9L.

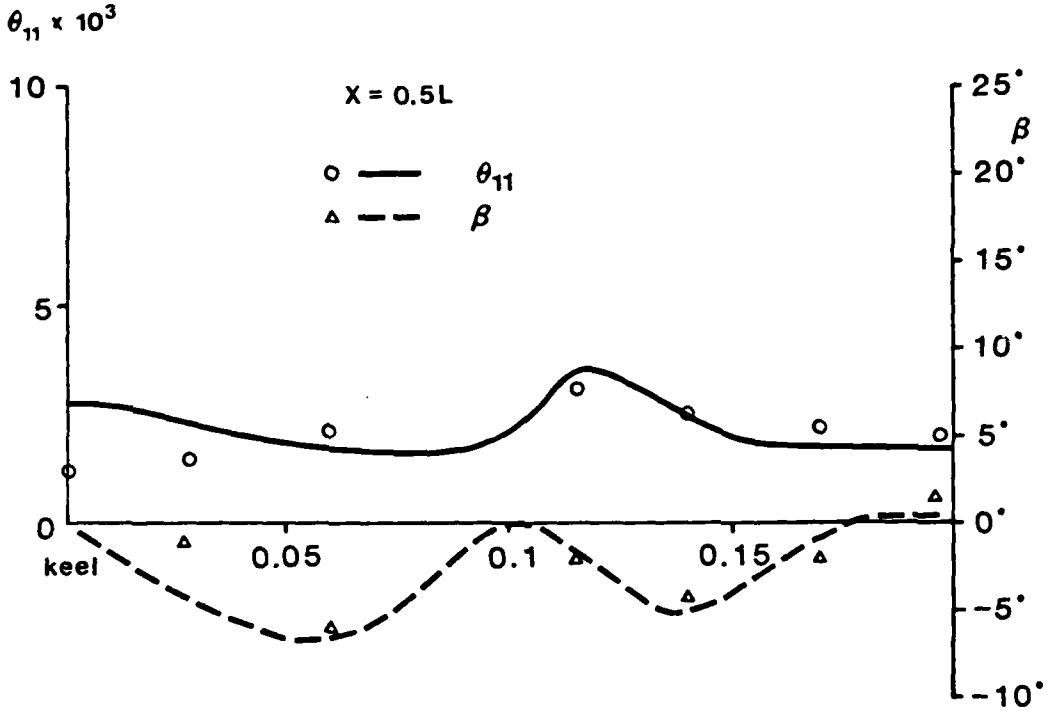

Figure 5. Comparison of the distribution along the cross-section of the computed and experimental values of the streamwise momentum thickness θ_{11} and the cross-flow angle β. In this figure the cross-section is at x = 0.5L.

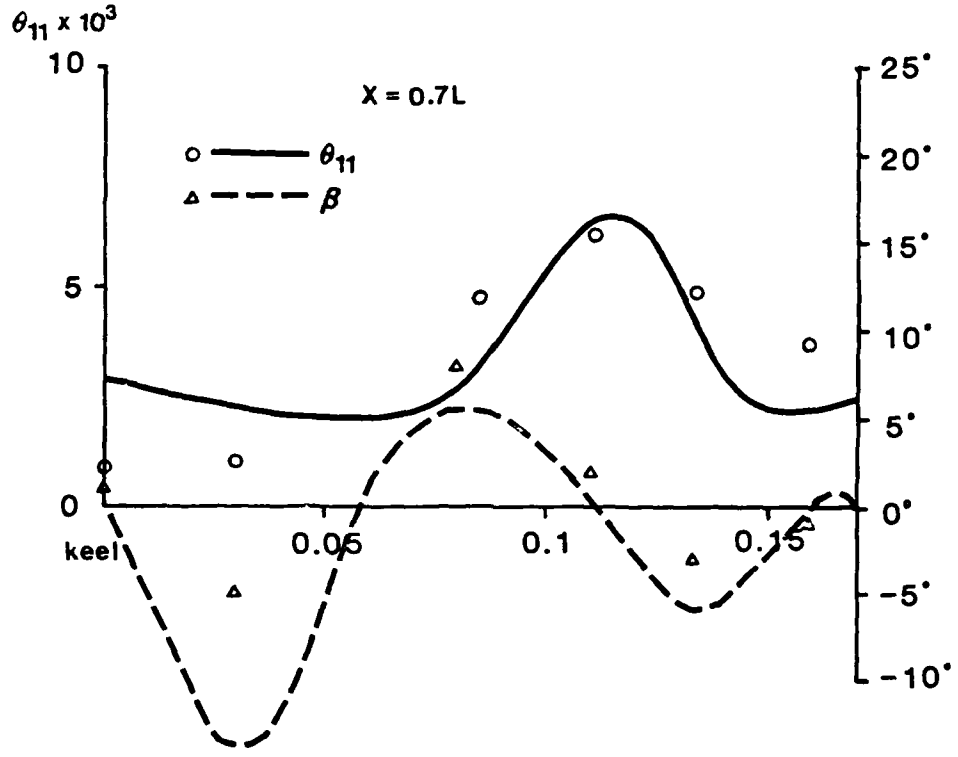

Figure 6. Comparison of the distribution along the cross-section of the computed and experimental values of the streamwise momentum thickness θ_{11} and the cross-flow angle β. The cross-section for this data is x = 0.7L.

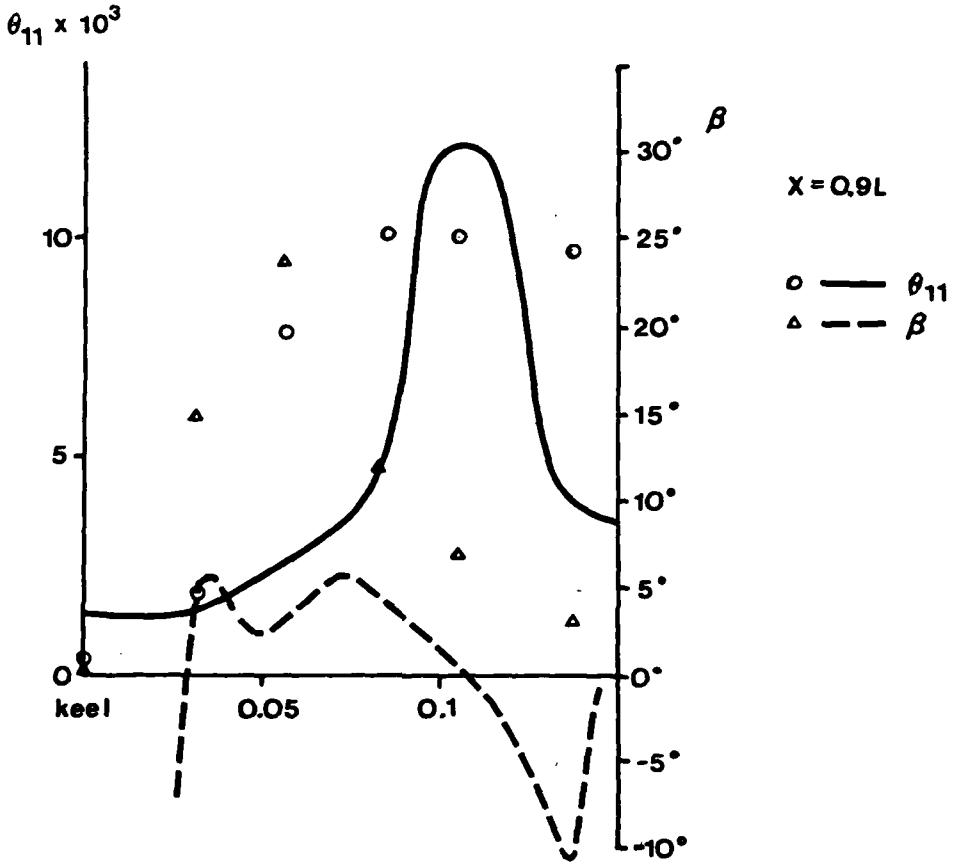

Figure 7. Comparison of the distribution along the cross-section of the computed and experimental values of the streamwise momentum thickness θ_{11} and the cross-flow angle β. The cross-section for this data is $x = 0.9_L$.

It is interesting to note that only one method tested in the SSPA-ITTC Workshop seemed to give substantially better results at station x = 0.9L than the present method. This was the differential method of Soejima, Yamazaki and Nakatake (see reference 7). This method made use of higher order boundary layer theory in which the viscous-inviscid interactions were accounted for. The results shown in Figures 6 and 7 do indicate that with the addition of viscous-inviscid interaction capabilities the present method may be capable of predicting well the boundary layer characteristics near the stern of a ship.

Viscous-inviscid interaction effects would tend to smooth the variation of the pressure distribution across the cross-sections. Thus the distribution of values of the boundary layer parameters would also be less variable across the cross-sections. This would be in accord with the experimental data shown in Figures 6 and 7.

Figures 8 and 9 show the profiles for the streamwise and cross-flow velocity at station x = 0.9L on streamline B and C. The computed profiles are not very accurate, but are at least in qualitative agreement with the experimental profiles. In particular, the cross-flow profile on streamline B is of the reversing (s shape) type. The lack of quantitative agreement between the computed and experimental velocity profiles should not be attributed to the formulas for the profile shapes. This lack of agreement is simply due to the fact that the boundary layer parameters θ_{11}, H and β were not predicted accurately enough at station x = 0.9L. It is believed that inclusion of the effects of viscous-inviscid interactions, not any basic change in the boundary layer cross-flow model, will bring the computed values of the boundary layer parameters into agreement with experimental values.

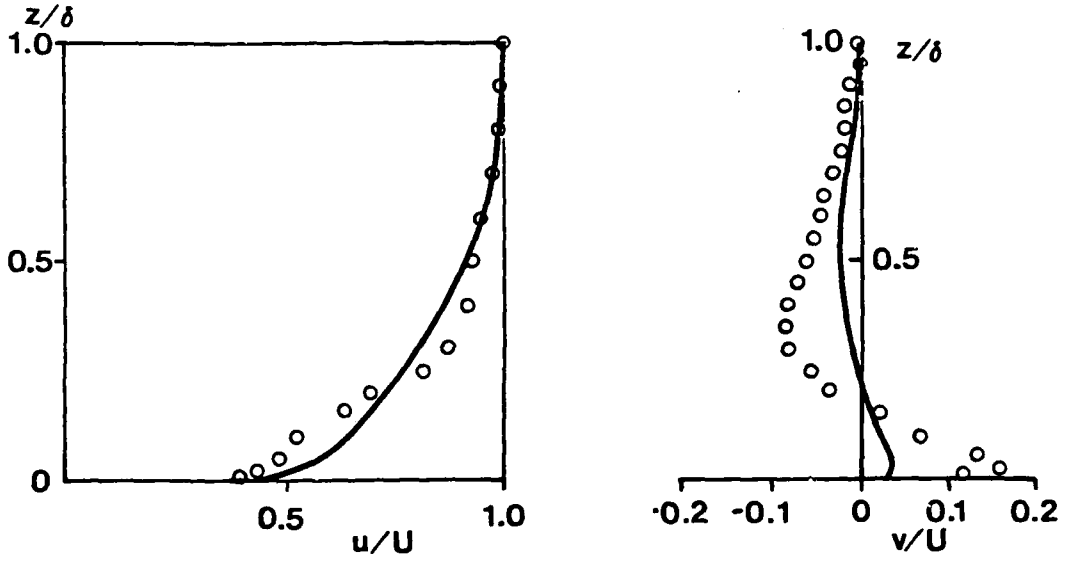

Figure 8. Comparison of the computed and experimental velocity profile on streamline B at station x = 0.9L. u/U is the velocity in the streamline direction and v/U is the velocity in the cross-flow direction. The curves are the computed profiles.

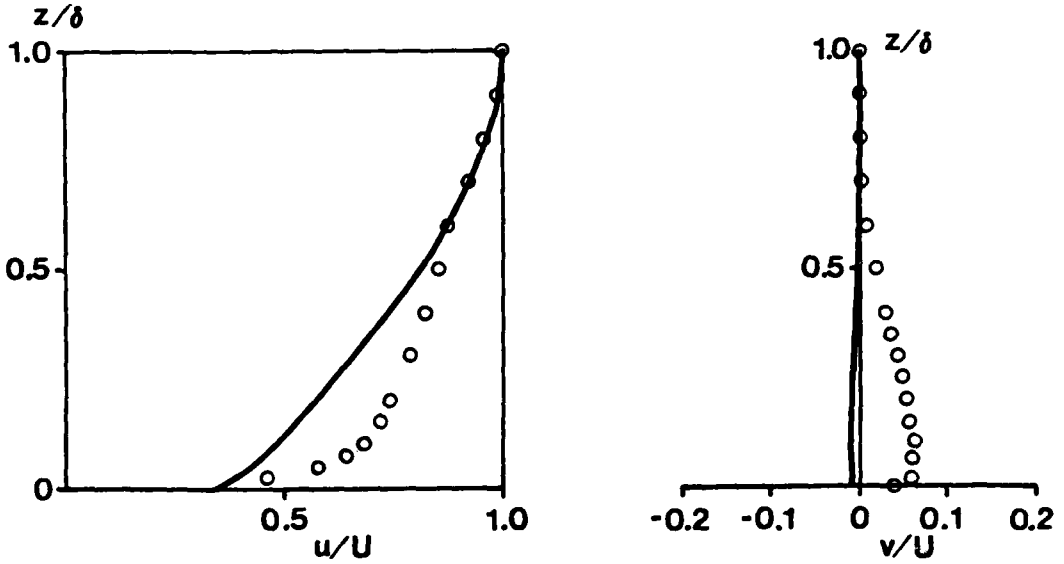

Figure 9. Comparison of the computed and experimental velocity profile on streamline C at station x = 0.9L. u/U is the velocity in the streamline direction and v/U is the velocity in the cross-flow direction. The curves are the computed profiles.

Section 7

CONCLUDING REMARKS

This report describes the development of a new three-dimensional momentum integral method of calculating ship boundary layers. It has been shown that the method does give reasonably good predictions of the boundary layer on the part of the ship where thin boundary layer theory is valid. The results of the test calculation near the stern, while not unreasonable, do require improvement. Such improvements will result by including viscous-inviscid interaction effects. The basic boundary layer model seems adequate.

The main accomplishment of this effort has been a fairly simple generalization of the Mager cross-flow model to include s-shaped profiles. What is needed now is to validate this model by further calculation of well-documented test cases. Such a program of calculations will help to establish the value of the constant (or possibly the function) c in equation (5) that relates the cross-flow angle β to the cross-flow pressure gradient K_2 and the momentum thickness θ_{21}.

Section 8

REFERENCES

1. von Kerczek, C., JSR, 17, pp. 106-120 (1973).

2. von Kerczek, C., & T. Langan, DTNSRDC Report 79/006 (July 1979).

3. Himeno, Y., & I. Tanaka, Tech. Reports Osaka U., Vol. 23, no. 1146, pp. 617-647 (1973).

4. Hatano, S., & T. Hotta, JSNA West Japan, 53, pp. 1-9 (1977).

5. Okuno, T., JSNA Japan, 139, pp. 10-23 (1976).

6. Larsson, L., Swedish State Shipbuilding Experimental Tank, Göteberg, Sweden, Report 47 (1974).

7. SSPA-ITTC Workshop on Ship Boundary Layers, SSPA Report 90 (1981).

8. Maoer, A., NACA Report 1067 (1952).

9. Eichelbrenner, E., AGARDograph 97, Pt. II, pp. 795-828 (1965).

10. Shanebrook, J., & D. Hatch, Trans. ASME, Ser. D: J. Basic Eng., 92, pp. 90-91 (1970).

11. Smith, P.D., ARC-R.&M. No. 3523 (1966).

12. Head, M.R., ARC-R.&M. No. 3152 (1960).

13. Kool, P., ZAMM, 59, pp. T277-T278 (1979).

14. von Kerczek, C., & E. Tuck, JSR, 13, pp. 284-298 (1969).

15. Isaacson, E., & H. Keller, Analysis of Numerical Methods, John Wiley & Sons, Inc., New York (1966).

INITIAL DISTRIBUTION

Copies

20 Commander
David W. Taylor Naval Ship
Research & Development Center
Attn: Code 1505, Bldg. 19, Rm. 129B
Bethesda, MD 20084

9 Commander
Naval Sea Systems Command
Washington, D.C. 20362
- 1 SEA 03R22 (J. Sejd)
- 1 SEA 312 (C. Kennel)
- 1 SEA 3213 (R. Keane, Jr.)
- 1 SEA 3213 (W. Sandberg)
- 1 SEA 05H (A. Paladino)
- 1 SEA 52
- 1 SEA 521 (F. Welling)
- 1 SEA 524 (P. Petros)
- 1 SEA 99612 (Library)

1 Dr. Robert E. Whitehead
Code 432
Office of Naval Research
800 N. Quincy Street
Arlington, VA 22217

2 Iowa Institute of Hydraulic Research
- 1 L. Landweber
- 1 V.C. Patel

1 Penn State Univ./ARL/B. Parkin

1 U. of Rhode Island/Dept. of Mech.
Eng./F.M. White

2 MIT/Dept. of Ocean Eng.
- 1 J. N. Newman
- 1 J. E. Kerwin

2 U. of Mich./Dept. of NAME
- 1 W. Vorus
- 1 R. Beck

1 Stevens Inst. of Tech./Davidson
Lab/J. Breslin

Copies

Copies	
2	U. of California/Berkeley 1 J. R. Pauling 1 W. C. Webster
1	U. of Washington/B. Adee
1	Webb Inst. of Nav. Arch./L. W. Ward
2	Hydronautics, Inc. 1 M. Tulin 1 O. Shearer

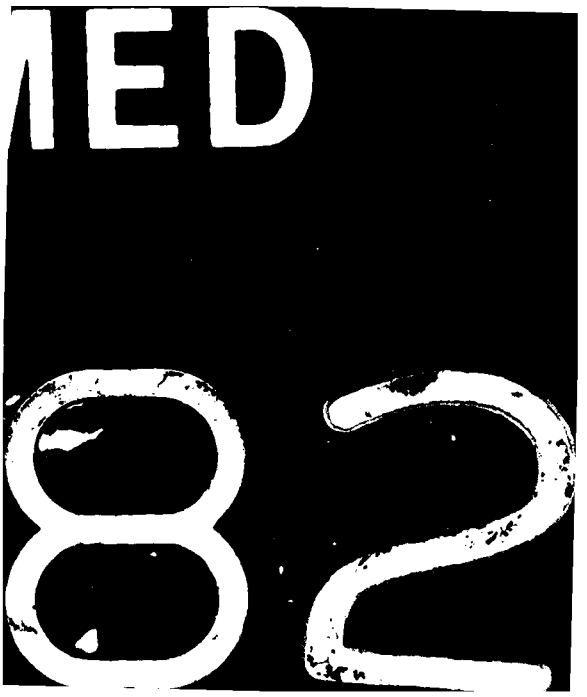
ED
82